Effects of Transition Metal Addition on the Solid-State Transformation of Molybdenum Trioxide to Molybdenum Carbides

Kyung Tack Jung, Won Bae Kim, Chang Houn Rhee, and Jae Sung Lee*

Department of Chemical Engineering and School of Environmental Science and Engineering, Pohang University of Science and Technology (POSTECH), San 31 Hyoja-dong, Pohang 790-784, Korea

Received May 15, 2003. Revised Manuscript Received November 5, 2003

Direct conversion of MoO_3 to molybdenum carbides by temperature-programmed reaction (TPR) with a reacting gas mixture of $CH_4/4H_2$ has been studied in the presence of a transition metal selected from Pt, Pd, Ni, Co, Cu, and pre-synthesized Mo_2C loaded on MoO_3. Loading of the metals reduced the temperatures of MoO_3 reduction and increased the specific surface area of produced carbides. However, the obtained phase of molybdenum carbides differed depending on the employed transition metal; Pt, Pd, or Ni produced cubic α-MoC_{1-x}, while Co, Cu, or pre-synthesized Mo_2C formed hexagonal β-Mo_2C, which was the same phase as that produced from the direct transformation of MoO_3 itself without any metal loading. The nature of transition metals loaded on MoO_3 also led to different TPR patterns for the transformation to molybdenum carbide, suggesting that different reaction routes were involved. Thus, MoO_3 loaded with Co, Cu, or Mo_2C showed TPR patterns similar to that of MoO_3 itself, except for slightly lower temperatures for the initiation of the reduction. With these metals, the transformation of MoO_3 to carbides followed a nontopotactic route involving the MoO_2 intermediate phase. By contrast, loading of Pt, Pd, or Ni to MoO_3 drove MoO_3 reduction into a topotactic transformation through a MoO_xC_y intermediate phase. However, unlike the well-established topotactic $MoO_3 \rightarrow Mo_2N \rightarrow \alpha-MoC_{1-x}$ transformation, the pseudomorphism was only partly maintained in this metal-promoted, direct $MoO_3 \rightarrow \alpha$-MoC_{1-x} transformation.

Introduction

The formation of metal carbides is extensive throughout the Periodic Table. All transition metals produce their corresponding carbides, revealing exceptions of the second and third rows of Group 9−10 metals (Rh, Ir, Pd, and Pt). In general, carbides of Group 4−6 metals are thermodynamically more stable and possess greatly improved catalytic properties over those of parent metals in activity, selectivity, and resistance to poisoning. Carbon atoms of these metal carbides reside in interstitial cavities between larger metal atoms.[1]

The carbides of Group 4−6 metals have been found to be good catalysts for a wide variety of reactions typically catalyzed by noble metals of high cost and limited supply. In particular, molybdenum carbides and nitrides have attracted attention as active and selective catalysts for reactions such as hydrogenation of CO or olefins,[2−6] NH_3 synthesis,[7] hydrocarbon reforming,[8,9] hydrogenolysis of hydrocarbons,[10,11] and hydrotreating.[12−16] Applicability of molybdenum carbides to practical catalysts requires high specific surface areas together with their effective structures. To prepare molybdenum carbides with high surface areas, the temperature-programmed reaction (TPR) method has been established; it induces the solid-state transformation of MoO_3 in a controlled manner by reacting MoO_3 with a nitrogen-containing reactive gas such as ammonia or a carbon-containing gas mixture such as CH_4/H_2.[17−21] The direct carburization of MoO_3 with CH_4/H_2

* Corresponding author. Tel: 82-562-279-2266. Fax: 82-562-279-5528. E-mail: jlee@postech.ac.kr.

(1) Lee, J. S.; Hyeon, T. Metal Carbides. In *Encyclopedia of Catalysis*; Horvath, I. T., Ed.; John Wiley & Sons: New York, 2003.
(2) Logan, M.; Gellman, A.; Somorjai, G. A. *J. Catal.* **1985**, *94*, 60.
(3) Leary, K. J.; Michaels, J. N.; Stacy, A. M. *J. Catal.* **1986**, *101*, 301.
(4) Ranhotra, G. S.; Haddix, G. W.; Bell, A. T.; Reimer, J. A. *J. Catal.* **1987**, *108*, 24.
(5) Lee, J. S.; Yeom, M. H.; Lee, D. S. *J. Mol. Catal.* **1990**, *62*, 145.
(6) Lee, J. S.; Yeom, M. H.; Park, K. Y.; Nam, I.; Chung, J. S.; Kim, Y. G.; Moon, S. H. *J. Catal.* **1991**, *128*, 126.
(7) Volpe, L.; Boudart, M. *J. Phys. Chem.* **1986**, *90*, 4874.
(8) Levy, R. B.; Boudart, M. *Science* **1973**, *181*, 547.
(9) Bridgewater, A. J.; Burch, R.; Michell, P. C. H. *J. Chem. Soc., Faraday Trans. 1* **1980**, *76*, 1811.
(10) Lee, J. S.; Locatelli, S.; Oyama, S. T.; Boudart, M. *J. Catal.* **1990**, *125*, 157.
(11) Iglesia, E.; Ribeiro, F. H.; Boudart, M.; Baumgartner, J. E. *Catal. Today* **1992**, *15*, 307.
(12) Lee, J. S.; Boudart, M. *Appl. Catal.* **1985**, *19*, 207.
(13) Abe, H.; Bell, A. T. *Catal. Lett.* **1993**, *18*, 1.
(14) Lee, K. S.; Abe, H.; Reimer, J. A.; Bell, A. T. *J. Catal.* **1993**, *139*, 34.
(15) Ramanathan, S.; Oyama, S. T. *J. Phys. Chem.* **1995**, *99*, 16365.
(16) Choi, J. G.; Brenner, J. R.; Thompson, L. T. *J. Catal.* **1995**, *154*, 30.
(17) Li, S. Kim, W. B.; Lee, J. S. *Chem. Mater.* **1998**, *10*, 1853.
(18) Volpe, L.; Boudart, M. *J. Solid State Chem.* **1985**, *59*, 332.
(19) Volpe, L.; Boudart, M. *J. Solid State Chem.* **1985**, *59*, 348.
(20) Lee, J. S.; Oyama, S. T.; Boudart, M. *J. Catal.* **1987**, *106*, 125.
(21) Lee, J. S.; Volpe, L.; Ribeiro, F. H.; Boudart, M. *J. Catal.* **1988**, *112*, 44.

10.1021/cm030395w CCC: $27.50
Published on Web 12/23/2003

produces a molybdenum carbide of the hcp structure β-Mo_2C, which is the thermodynamically stable phase under the preparation conditions. The nitride (fcc γ-Mo_2N) produced from the TPR of MoO_3 with NH_3 is transformed to the carbide by TPR with CH_4/H_2.[21] However, the carbide obtained via the nitride shows the metastable fcc α-MoC_{1-x} phase. This $MoO_3 \rightarrow Mo_2N \rightarrow \alpha$-$MoC_{1-x}$ transformation has been established to be *topotactic* since the crystallographic motif is conserved in these three molybdenum phases by minimal movement of molybdenum atoms throughout the whole solid transformation. The platelet morphology of MoO_3 is also conserved in Mo_2N and α-MoC_{1-x} (pseudomorphism). The direct carburization by ethane/H_2 as a reacting gas mixture lowers the required synthesis temperature and increases the surface area of the final carbides compared to those prepared with CH_4/H_2.[22] Yet product powders showed the hcp β-Mo_2C phase. The sonochemical decomposition of molybdenum hexacarbonyl produced fcc α-MoC_{1-x}, with a high surface area of 180 $m^2\ g^{-1}$.[23−25] Impregnation with a small amount of Pt (0.25 wt %) to MoO_3 produced high surface area α-MoC_{1-x} by direct TPR/carburization, which was pseudomorphous with MoO_3.[21] Thus, the nature of the solid transformation from MoO_3 to molybdenum carbides is dictated by the preparation conditions and products with different structures, surface areas, and morphologies are formed.[17,21,26]

This work investigates the effect of various transition metals on the solid-state transformation of MoO_3 to molybdenum carbides under a CH_4/H_2 gas stream. A small amount of Group 9−11 metals (0.2−0.3 wt %) was loaded on the bulk MoO_3 before the gas−solid reactions. The morphology, crystal structure, and physicochemical surface properties of obtained molybdenum carbides are examined by X-ray diffraction (XRD), scanning electron microscopy (SEM), N_2 adsorption and CO chemisorption, and TPR profiles.

Experimental Section

Preparation of Molybdenum Carbides. *Impregnation of Transition Metals on MoO_3.* Bulk MoO_3 (Alfa, 99.95%) was impregnated with an aqueous solution of a transition metal precursor by an incipient wetness method, followed by drying the slurry to remove water in an oven at 383 K for 20 h. A description of the metal precursors employed here is listed in Table 1 together with the amount of the precursors in weight percent of metal to MoO_3. A physical mixture of MoO_3 and a pre-synthesized Mo_2C was also prepared to examine a possible role of Mo_2C in MoO_3 transformation.

Temperature-Programmed Reaction (TPR). A temperature-programmed reaction of the metal-loaded molybdenum trioxide was employed to prepare molybdenum carbide powders with high surface areas and the solid-state transformation processes were investigated by observation of gas evolution. Detailed conditions of TPR have been described in previous works.[17−21] To prepare fcc α-MoC_{1-x} as a reference, we employed two consecutive steps of nitridation of MoO_3 with NH_3 to Mo_2N, followed by carburization of the nitride to α-MoC_{1-x} under a CH_4/H_2 gas stream.

Table 1. Transition Metals Employed for the Solid-State Transformation of MoO_3 under a CH_4/H_2 Gas Stream

metal	amount of loading (wt %, based on Mo)	precursor employed
Co	0.2	$Co(NO_3)_2 \cdot 6H_2O$ (Janssen, 99%)
Cu	0.2	$Cu(NO_3)_2 \cdot xH_2O$ (Aldrich, 99.999%)
Mo_2C[a]	1.0	hcp phase β-Mo_2C
Ni	0.2	$Ni(NO_3)_2 \cdot 6H_2O$ (Aldrich, 99.999%)
Pd	0.2	$Pd(NO_3)_2 \cdot 2H_2O$ (Sigma)
Pt	0.3	$H_2PtCl_2 \cdot 6H_2O$ (Aldrich, 99.995%)

[a] Physical mixture of bulk MoO_3 and 1 wt % hcp phase β-Mo_2C, which had been prepared from MoO_3, as described in the Experimental Section.

For the TPR of the metal-loaded MoO_3, 80 mg of the sample powder was used in a U-shaped quartz reaction cell with an outer diameter of 13 mm. This cell was equipped with two stopcocks at the inlet and outlet parts of gas flow, which enabled the produced molybdenum carbides to be characterized in situ without exposure to the atmosphere after the TPR. The employed gases were CH_4 (Union Carbide, 99.95%) and H_2 (KBOC, 99.99%) for reduction and carburization. These gases were further purified by passing through a 5-Å molecular sieve trap and an oxygen trap (Alltech). NH_3 (Matheson, 99.99%) was used to prepare the intermediate phase of molybdenum nitride. A stream of gas mixture was passed through the reaction cell at a total flow rate of 37 μmol s^{-1} with a mixing ratio of 1/4 for CH_4 to H_2. The temperature was varied in a furnace coupled with a PID controller and monitored locally with a thermocouple. The temperature increased at a ramping rate of 5 K min^{-1} from 373 to 1173 K. Identification and analysis of gaseous reaction products were performed by an online mass spectrometer (HP 5972).

Characterization Methods. *Structure and Morphology.* Since fresh molybdenum carbide powders burn spontaneously upon exposure to air, samples were passivated prior to the characterization by letting 0.5% O_2 in He pass through the produced powder for 2 h, followed by letting the air diffuse slowly into the reaction cell through one end of the reactor open to atmosphere for 20 h. This passivation procedure allowed the final samples subject to a mild surface oxidation without the structural and morphological change of bulk molybdenum carbides.

To examine the structural change after and during the TPR, powder X-ray diffraction (XRD) measurements were conducted using a Mac Science M18XHF diffractometer with Cu Kα radiation (λ = 1.5405 Å). The morphology of the passivated samples was observed by scanning electron microscopy (SEM) on a Hitachi S-2460N.

Measurements of Surface Area and Mo Dispersion. The CO chemisorption and N_2 adsorption were conducted on a conventional volumetric adsorption apparatus without exposure of the sample to atmosphere after the TPR by use of the stopcocks attached on the reaction cell. Before measurement of CO uptake, the reaction cell containing the powder sample was evacuated to a pressure less than 10^{-4} Pa for 0.5 h and the reaction cell was cooled to room temperature. Then the first CO adsorption isotherm was taken as CO pressure increased. At room temperature, the cell was again evacuated to a pressure less than 10^{-4} Pa for 0.5 h to remove physisorbed CO. The second isotherm was taken in a similar way, and the amount of irreversible CO uptake was obtained from the difference between the two isotherms extrapolated to zero pressure. The specific surface areas (S_g) of the samples were determined by the BET method from N_2 adsorption at 77 K on the same adsorption apparatus.

Results

TPR Profiles of Transition Metal-Loaded MoO_3. Solid-state transformation of molybdenum trioxide into molybdenum carbides by reaction with a reactive gas mixture of $CH_4/4H_2$ involves generally two consecutive

(22) Claridge, J. B.; York, A. P. E.; Brungs, A. J.; Green, M. L. H. *Chem. Mater.* **2000**, *12*, 132.
(23) Suslick, K. S.; Choe, S. B.; Cichowlas, A. A.; Grinstaft, M. W. *Nature* **1991**, *353*, 414.
(24) Suslick, K. S.; Hyeon, T.; Fang, M. *Chem. Mater.* **1996**, *8*, 2172.
(25) Li, S.; Lee, J. S.; Hyeon, T.; Suslick, K. S. *Appl. Catal. A* **1999**, *184*, 1.
(26) Volpe, L.; Boudart, M. *Catal. Rev.-Sci. Eng.* **1985**, *27*, 515.

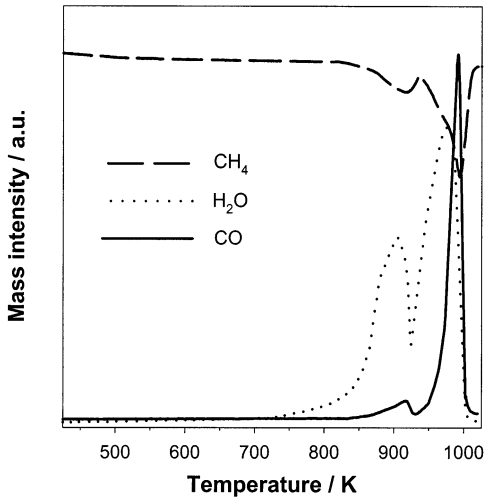

Figure 1. Temperature-programmed reaction profiles of the transformation of MoO_3 in a $CH_4/4H_2$ stream (ramping rate = 300 K h^{-1}, MoO_3 loading = 80 mg, flow rate = 37 μmol s^{-1}).

processes; the reduction of MoO_3 to MoO_2 by H_2 at a relatively low temperature without involving CH_4, followed by the simultaneous further reduction and carburization of the intermediate MoO_2 to molybdenum carbides by reaction with both methane and dihydrogen.[17] Figure 1 represents a typical temperature-programmed reaction (TPR) profile of the transformation of molybdenum trioxide to its carbide under the $CH_4/4H_2$ stream. There are two H_2O formation peaks at ca. 900 K and ca. 970 K and peaks due to the consumption of CH_4 and production of CO above 850 K. We also observed CO_2 formation at a temperature similar to that of CO formation, but this profile was excluded because its amount was negligible. In the second reduction step, CH_4 seemed to serve as both reduction and carburization agents. Carbon and hydrogen atoms in CH_4 should contribute to the reduction of MoO_2 produced from the first reduction step as carbon converts to CO and CO_2 and hydrogen to H_2O. At the same time carbon atoms are incorporated into molybdenum lattice. This TPR pattern of MoO_3 itself by a $CH_4/4H_2$ stream was in line with the previous work.[17]

We investigated the effects of the transition metal loading (less than 0.3 wt % of Mo) on the direct solid-state transformation of MoO_3 into the carbides. Figure 2 illustrates the TPR profiles for the transformation of

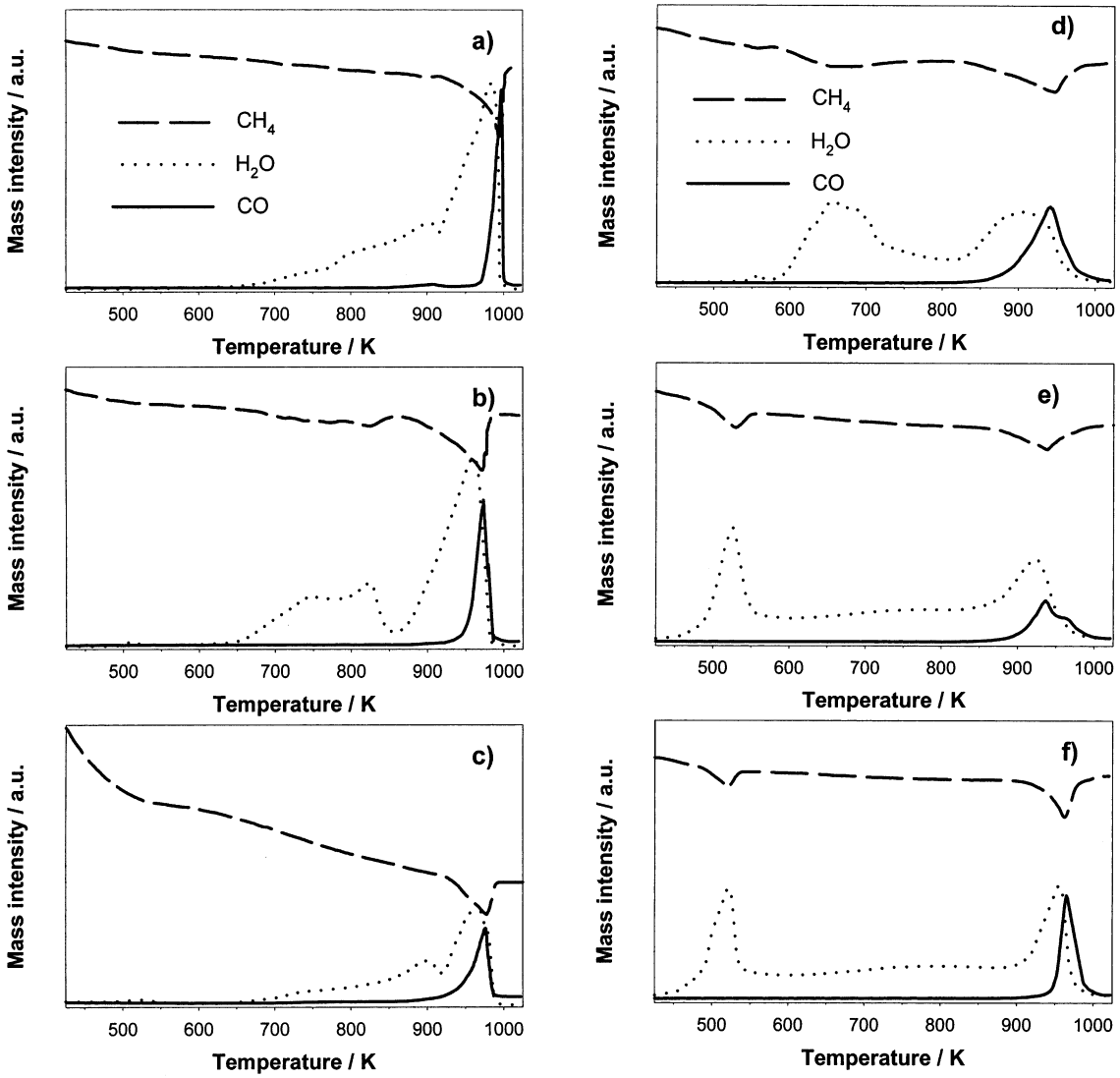

Figure 2. Temperature-programmed reaction profiles of the transformation of (a) Co-, (b) Cu-, and (c) Mo_2C-loaded MoO_3 with a $CH_4/4H_2$ stream (ramping rate = 300 K h^{-1}, MoO_3 loading = 80 mg, flow rate = 37 μmol s^{-1}). (d) Ni-, (e) Pd-, and (f) Pt-loaded MoO_3 with a $CH_4/4H_2$ stream (ramping rate = 300 K h^{-1}, MoO_3 loading = 80 mg, flow rate = 37 μmol s^{-1}).

MoO_3 loaded with Co, Cu, a pre-synthesized Mo_2C, Ni, Pd, or Pt. The initial temperature of H_2O formation appeared at lower temperatures by 100−250 K in all cases than that of the TPR profile of MoO_3 itself shown in Figure 1. In addition to the decrease in the starting temperature of the first reduction stage, the final transformation temperature at 950−1000 K was also lowered by at least 50 K in the TPR profiles for Cu, Ni, Pd, and Pt-loaded MoO_3. Furthermore, it should be noted that the metals of the Group 10 (Ni, Pd and Pt) showed profiles similar to each other in the H_2O formation pattern, with the first reduction occurring below 650 K. These patterns are distinguished from those for Co, Cu, and Mo_2C that showed the first reduction temperatures above 700 K.

The consumption peaks of CH_4 gave a more interesting feature. In TPR of Pd- and Pt-loaded MoO_3 shown in Figure 2, parts (e) and (f), there were two sharp CH_4 consumption peaks that accompanied two H_2O formation peaks. The Ni-loaded MoO_3 (Figure 2d) did not show such sharp peaks, especially for the low-temperature CH_4 consumption, but the pattern seemed to be qualitatively the same as those for Pd and Pt. However, there was no indication for the production of carbon-containing gas molecules such as CO and CO_2 at these low temperatures in all cases, suggesting that carbons produced from methane would reside in MoO_3 without forming any gas molecules. By contrast, Figure 2, parts (a)−(c), showed no indication of such carbon incorporation at low temperatures in MoO_3 loaded with Co, Cu, and Mo_2C.

Structure and Morphology of Molybdenum Carbides and Their Intermediates. The powder XRD patterns of reactant and product solids are presented in Figure 3. The Mo_2C (hcp) was produced from one-step TPR of MoO_3, and MoC_{1-x} (fcc) from two-step TPR, that is, the first TPR of MoO_3 with NH_3 to form the nitride intermediate fcc Mo_2N, followed by TPR of Mo_2N with $CH_4/4H_2$. The X-ray diffraction (XRD) pattern of MoO_3 reveals the greatly enhanced peak intensities of {0*k*0} planes such as (020), (040), and (060), indicating an anisotropic platelet structure. The scanning electron microscopy (SEM) image in Figure 4a confirms this morphology of the platelet structure. However, the strong {101} peaks of Mo_2C imply that the morphology has been changed by breaking the {0*k*0} planes, as confirmed again by its SEM micrograph in Figure 4c that showed mostly agglomerated isotropic particles that were completely different from the morphology of its parent MoO_3. In cases of Mo_2N and MoC_{1-x}, however, the XRD patterns represent intense peaks for {200} planes that are parallel to the {0*k*0} planes of MoO_3, suggesting that the topotactic phase transformation was involved from MoO_3 to Mo_2N and from Mo_2N to MoC_{1-x}. The intensity distribution of XRD peaks and the pseudomorphism are consequences of the topotactic or nontopotactic phase transformations of $MoO_3 \rightarrow Mo_2N \rightarrow MoC_{1-x}$ and $MoO_3 \rightarrow Mo_2C$, respectively. The structures of molybdenum carbides produced from the metal-loaded MoO_3 were examined by XRD. Figure 5 shows two different structures of the carbides obtained: fcc MoC_{1-x} from Ni, Pd- and Pt-loaded MoO_3, and hcp Mo_2C from Co-, Cu-, and Mo_2C-loaded MoO_3. The relative intensity of (200) to (111) peaks for this MoC_{1-x} was

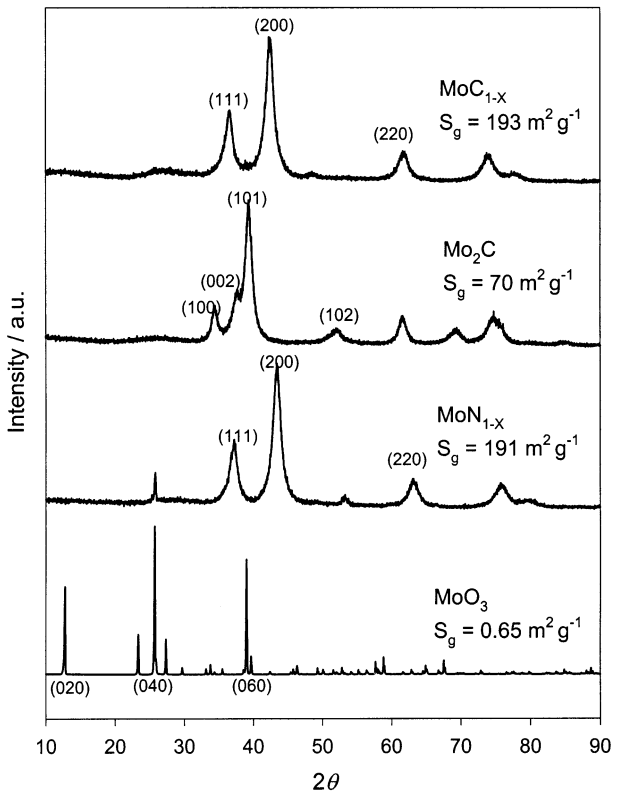

Figure 3. XRD patterns showing the structural evolution for topotactic and nontopotactic transformations of MoO_3 to molybdenum nitride and carbides.

lower than that for MoC_{1-x} produced via molybdenum nitride shown in Figure 3, but closer to a theoretical intensity ratio for isotropic fcc crystals.[21] This different intensity distribution of XRD peaks for two types of MoC_{1-x} could be understood when observing SEM images of Figure 6 that show morphologies of all carbides produced from metal-loaded MoO_3.

For the hcp Mo_2C produced from Co, Cu, and Mo_2C-loaded MoO_3 shown in Figure 6a−c, most of the large platelet particles were broken into smaller ones and numerous agglomerates of small particles could be observed. These morphologies, however, are different from that of Mo_2C prepared without transition metal loading in that there are many nonisotropic platelet particles, although they are smaller in size than original MoO_3 particles. The morphology of MoC_{1-x} obtained from Ni-, Pd-, and Pt-loaded MoO_3 in Figure 6d−f showed no agglomerates of particles but instead showed mostly broken platelets. The shape of the original large platelets of MoO_3 still remained for Ni- and Pd-loaded MoC_{1-x}. However, it appeared that the anisotropy manifested by these broken MoC_{1-x} platelets was not extensive enough to cause the unusual intensity distribution of XRD peaks as observed for MoC_{1-x} prepared via Mo_2N.

Figure 7 represents the structural evolution of molybdenum species involved in the reduction/carburization process of metal-loaded MoO_3. These XRD patterns were obtained for the samples after TPR had been stopped and quenched at the indicated temperatures. The temperatures to quench the TPR were chosen to be the points where the first-stage reduction was finished by referring to the TPR patterns of Figure 2. The Co- and Cu-loaded samples showed XRD patterns

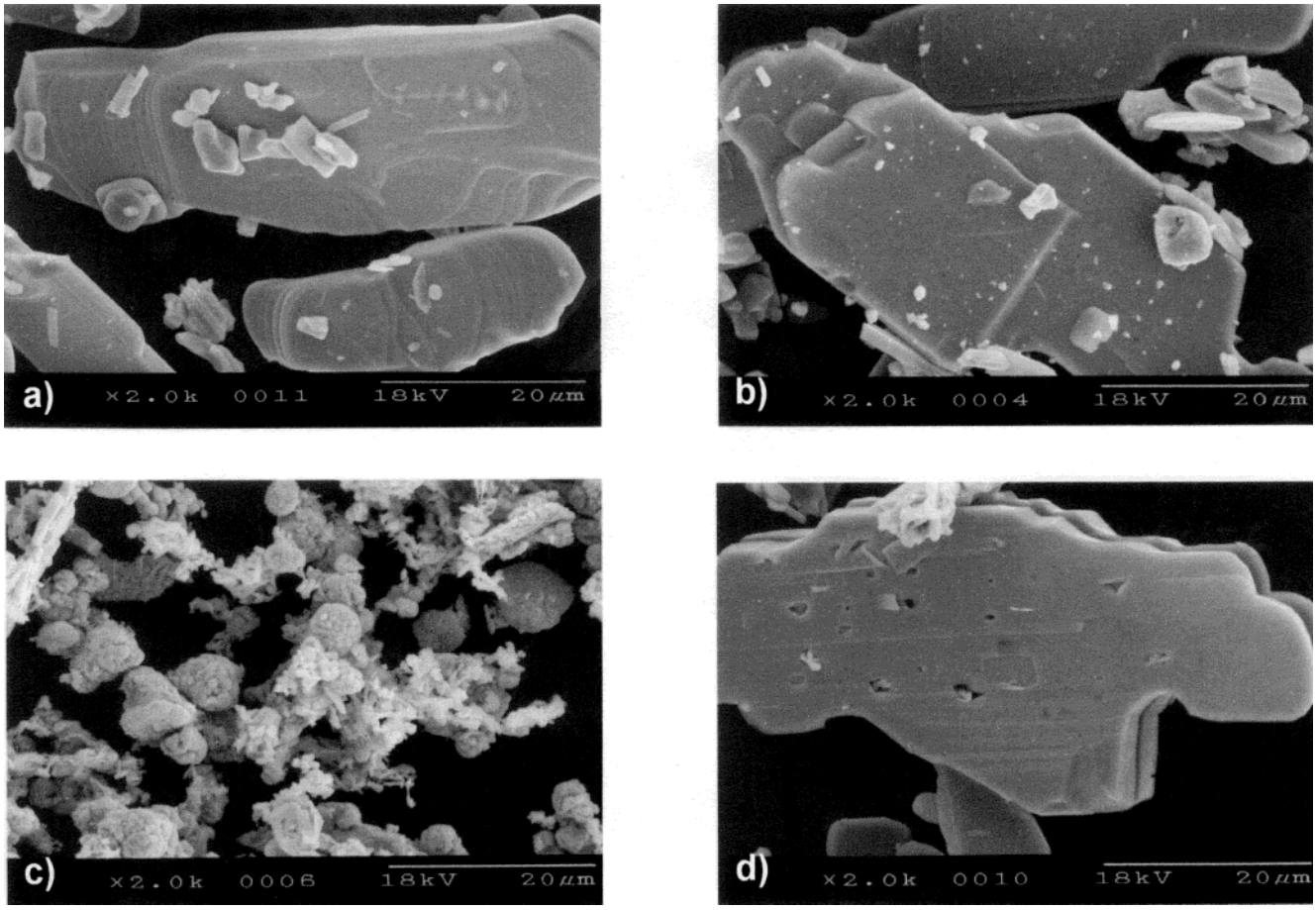

Figure 4. Morphology of (a) MoO_3, (b) Mo_2N, (c) Mo_2C, and (d) MoC_{1-x} observed by SEM with a magnification of 2000.

exclusively of MoO_2. The Mo_2C-loaded MoO_3 also showed MoO_2 as a dominant species together with Mo_4O_{11}, which was less reduced than MoO_2. In contrast, a molybdenum oxycarbide, MoO_xC_y, appeared during the carburization of Ni-, Pd-, and Pt-loaded MoO_3. Although a rather small contribution of the oxycarbide intermediate was observed for Ni, its formation was dominant for the Pd- and Pt-loaded cases.

Surface Properties of Molybdenum Carbides. Table 2 shows the results of N_2 adsorption and CO chemisorption on the molybdenum carbides produced in the present work. Adsorption was conducted in situ without exposure of the sample to air. In all cases of the metal loading, substantial increases of the specific surface area (S_g) were observed for the produced molybdenum carbides no matter what their final structure was, compared to that of Mo_2C produced from bare MoO_3 (70 $m^2\ g^{-1}$). The Cu-loaded molybdenum carbide showed the highest surface area of 221 $m^2\ g^{-1}$. These S_g values were consistent with the X-ray line broadening in that XRD peaks became broader for metal-loaded Mo_2C (Figure 5) relative to those of bare Mo_2C (Figure 3). As the surface area increased, the greater amount of irreversible uptake of CO was observed. In general, the samples with lower starting temperatures of the reduction in their TPR profiles possessed higher surface areas as well as greater amounts of CO chemisorption.

Table 2 also lists properties of MoC_{1-x} produced by two-step topotactic routes, that is, nitridation of MoO_3 to Mo_2N, followed by carburiztion of Mo_2N to MoC_{1-x}. The latter showed a high surface area of ca. 190 $m^2\ g^{-1}$ or larger. Except for Mo_2C-loaded Mo_2C, the other

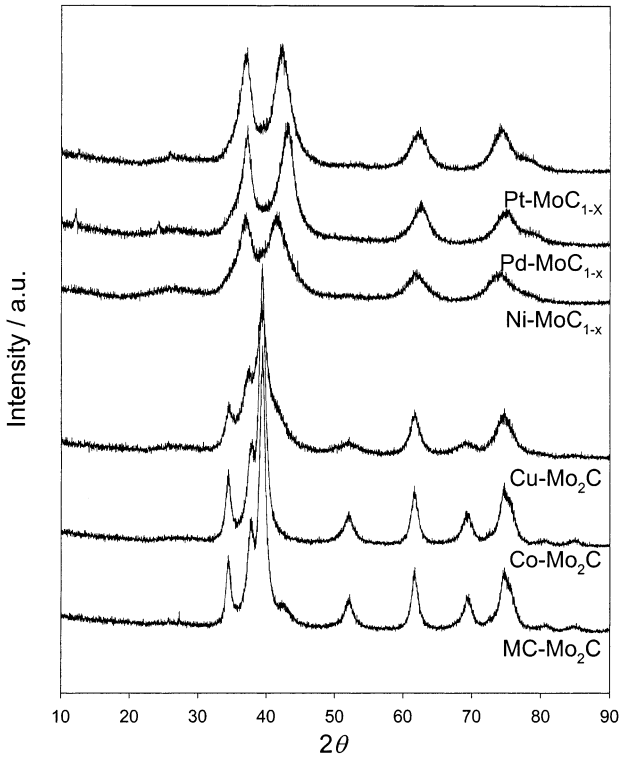

Figure 5. XRD patterns of metal-loaded molybdenum carbides. Note that fcc MoC_{1-x} phase is dominant for Ni-, Pd-, and Pt-loaded samples and hcp Mo_2C phase is dominant for Mo_2C-, Co-, and Cu-loaded molybdenum carbides.

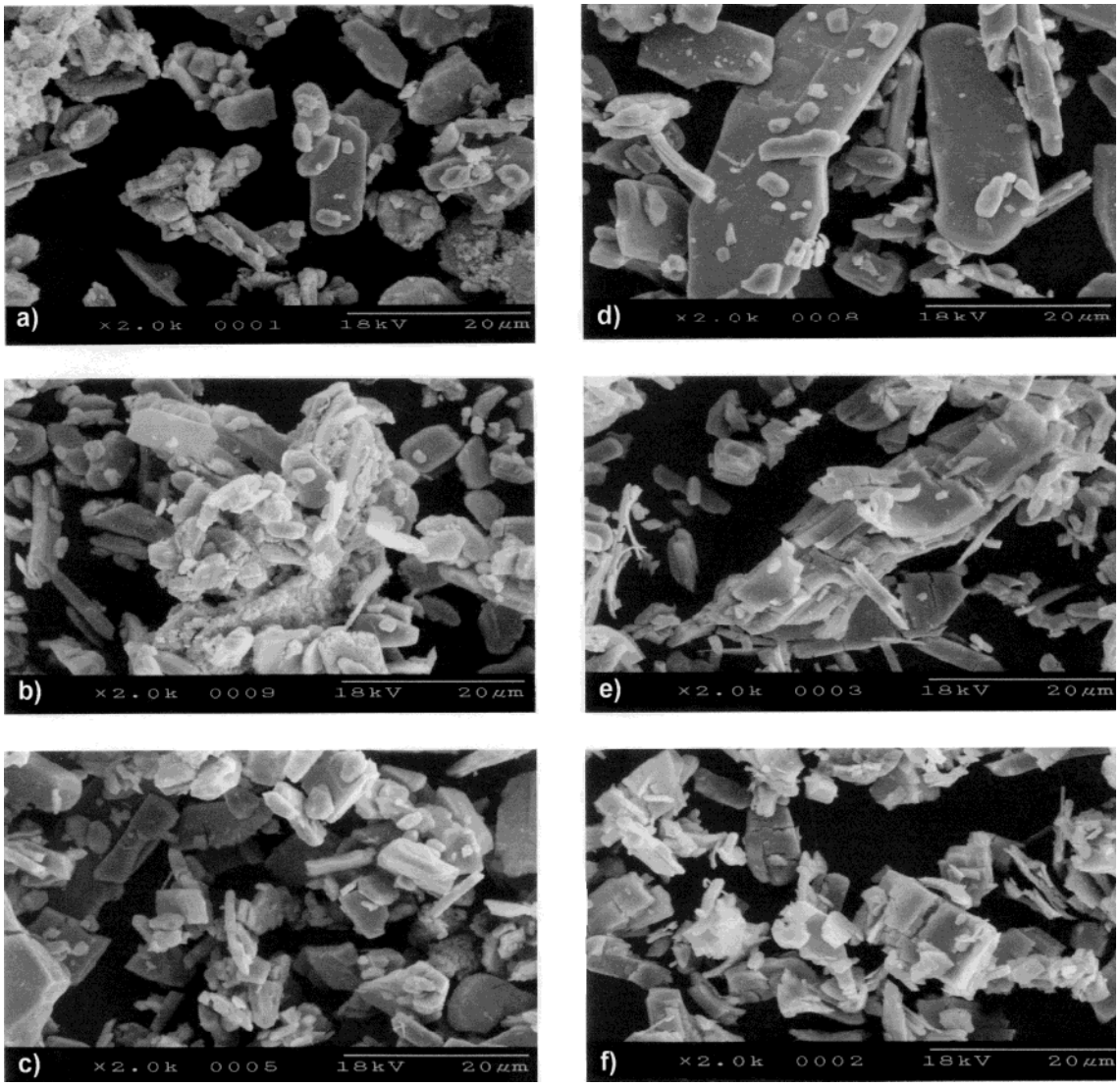

Figure 6. Morphology of (a) Co-, (b) Cu-, and (c) Mo_2C-loaded molybdenum carbides observed by SEM with a magnification of 2000. (d) Ni-, (e) Pd-, and (f) Pt-loaded molybdenum carbides observed by SEM with a magnification of 2000.

metal-loaded molybdenum carbides had a comparable or slightly higher S_g than that of MoC_{1-x}. More interestingly, metal-loaded MoC_{1-x} samples showed amounts of CO chemisorption greater by 80−120 μmol g^{-1} for Ni−, Pd−, and Pt−MoC_{1-x}, compared to that of bare MoC_{1-x} (540 μmol g^{-1}). This is reflected in the great increase of areal number density for these materials by up to 25%. A possible chemisorption of CO on the added metal itself could be ignored unambiguously by following a simple calculation. Even if all the added metals were exposed by 100% dispersion on the surface of MoC_{1-x}, their amount would be 34, 19, and 15 μmol, respectively, for Ni, Pd, and Pt. Thus, the maximum contribution of CO chemisorbed on these metals is less than 5% of the total amount of CO actually chemisorbed on Ni-, Pd-, and Pt-loaded MoC_{1-x}. The increased CO site densities for metal-loaded molybdenum carbides appears to originate from the surface-cleaning effect of loaded transition metals. A part of the molybdenum carbide surface is covered with unreactive "graphitic" carbon that comes from the preparation step and blocks CO adsorption sites.[20] Transition metals could hydrogenate this surface carbon off the molybdenum carbide surface.

Discussion

The molybdenum carbide with the fcc structure α-MoC_{1-x} has been known to possess higher specific surface areas (∼200 m^2 g^{-1}) than those with the hcp structure Mo_2C (∼70 m^2 g^{-1}). This fcc phase is usually prepared through a topotactic route of MoO_3 → Mo_2N → α-MoC_{1-x} transformation. In this study, we have demonstrated that the α-MoC_{1-x} phase of similar properties could be synthesized by one-step reduction/carburization of MoO_3 in the presence of a transition metal (Ni, Pd, or Pt) loaded on MoO_3 prior to TPR with CH_4/H_2. When Cu, Co, or pre-synthesized Mo_2C is loaded instead on MoO_3, the hcp Mo_2C phase is obtained as in the absence of any transition metal. However, this metal-loaded Mo_2C possesses the high surface areas comparable with those for α-MoC_{1-x}. The S_g values for Cu- and Co-loaded Mo_2C are close to 200 m^2 g^{-1}. To the best of our knowledge, these are, by far, the highest surface areas reported for bulk Mo_2C. Thus, employment of transition metals in the preparation of molybdenum carbides exerts one of two effects depending on the nature of the metal: to provide a direct synthesis route to metastable α-MoC_{1-x} phase or to the usual

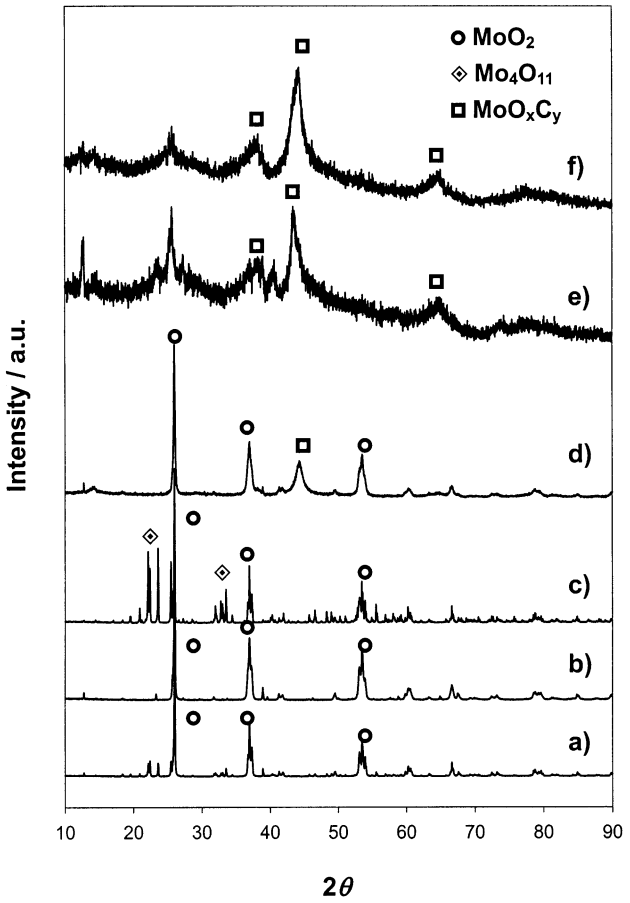

Figure 7. XRD patterns showing the structural evolution of intermediate species during the carburization of the metal-loaded MoO_3 by $CH_4/4H_2$. These molybdenum intermediates were observed after the TPR was stopped and the sample was quenched at 913 K for (a) Co-, (b) Cu-, and (c) Mo2C-loaded MoO_3 and at 793 K for (d) Ni-, (e) Pd-, and (f) Pt-loaded MoO_3.

Table 2. Physicochemical Properties of the Bare and the Metal-Loaded Molybdenum Carbides

sample	S_g[a] ($m^2\ g^{-1}$)	amount of CO chemisorbed[b] ($\mu mol\ g^{-1}$)	number density[c] ($10^{18}\ m^{-2}$)	XRD phase[d]
Mo_2C	70	164	1.41	hcp
$Co-Mo_2C$	182	565	1.87	hcp
$Cu-Mo_2C$	221	602	1.64	hcp
$MC-Mo_2C$	122	209	1.03	hcp
MoC_{1-x}	193	540	1.68	fcc
$Ni-MoC_{1-x}$	209	662	1.91	fcc
$Pd-MoC_{1-x}$	180	620	2.07	fcc
$Pt-MoC_{1-x}$	178	620	2.10	fcc

[a] Specific surface area determined by N_2-BET method. [b] Amount of CO adsorbed irreversibly on the surface of molybdenum carbides. [c] Areal number density of molybdenum metal sites titrated by CO chemisorption under an assumption of one-to-one adsorption of CO to the exposed metal. [d] Dominant phase examined by XRD.

Mo_2C phase but with greatly increased surface areas. The second effect is of significant importance when the material is used for the catalyst for a structure-sensitive reaction. For example, the *n*-butane hydrogenolysis at 510 K proceeds over Mo_2C with turnover rates more than 10 times higher than those over α-MoC_{1-x}.[10]

The common feature of the metal-promoted carbide synthesis is the high surface areas of the obtained solid products relative to Mo_2C obtained without a loaded metal. This great increase in surface area might be attributed to the lower temperatures at which the reduction of MoO_3 is initiated. The reduction started at about 650−700 K by showing the evolution of H_2O for MoO_3 loaded with Cu, Co, or Mo_2C. However, the reduction was initiated at about 800 K for MoO_3 itself; thus, the metal loading lowered the reduction temperature by 100−150 K. The crystal growth of Mo_2C particles should be determined by the mobility of metal atoms such as in other metal-sintering processes. At the initial reduction temperature of MoO_3, oxygen atoms start to diffuse out of MoO_3 lattice, which would cause significant movement of molybdenum atoms as well. The extent of the movement should depend on the reduction temperature. Thus, low reduction temperatures limit the mobility and lead to small particles with high surface areas. Still, loading of these metals did not change the obtained molybdenum carbide phase, producing hcp Mo_2C phase with and without the added metals.

The loading of metals such as Ni, Pd, or Pt to MoO_3 reduced the initial reduction temperature further down to 450 K and now the solid-transformation process became topotatic, leading to the formation of the metastable fcc α-MoC_{1-x} phase. This initial reduction temperature is similar to the temperature observed for the MoO_3 reduction with NH_3.[10,18] It is well-known that transition metals catalyze the reduction of MoO_3 by activating the reducing agent, dihydrogen.[27] Apparently, this catalytic effect by Ni, Pd, and Pt is higher than that by Cu, Co, and Mo_2C.

The reduction of MoO_3 by H_2 in the presence of Ni, Pd, and Pt starts from forming a hydrogen bronze, H_x-MoO_3, even at room temperature.[19,28−30] This hydrogen bronze is produced via hydrogen spillover from the transition metal surface to MoO_3.[27] This stage of reaction gives no TPR signal because it does not produce any gaseous molecule. Upon further heating, water is produced and methane is consumed as indicated in TPR spectra of Figure 2d−f. The XRD patterns after this stage of reduction indicate that an oxycarbide intermediate of an fcc structure (MoO_xC_y)[31] has been formed. At the same stage of reduction of MoO_3 without any metal or with Cu, Co, and Mo_2C, MoO_2 and other suboxides are formed as solid intermediates. In this case, there is no indication of carbon incorporation into the molybdenum by methane decomposition. Thus, it appears that the oxycarbide is the intermediate for topotactic MoC_{1-x} formation, whereas MoO_2 is that for nontopotactic Mo_2C formation. This is in line with the formation of oxynitride intermediates in the topotactic reduction/nitridation of MoO_3 to Mo_2N by NH_3.[17,18]

The key requirement for the topotactic solid transformation is the conservation of a structural motive usually maintained by the relative position of metal atoms.[26] When MoO_3 starts to be reduced, the structural motive would be disturbed by departure of oxygen atoms. If the reduction continues, the stable MoO_2 phase

(27) Sermon, P. A.; Bond, G. C. *Catal. Rev.* **1973**, *8*, 211.
(28) Fripiat, J. J. *Surface Properties and Catalysis by Non-metals*; Bonelle, J. P., Delmon, B., Derouane, E., Eds.; Reidel Publishing: Boston, 1983.
(29) Vannice, M. A.; Boudart, M.; Fripiat, J. J. *J. Catal.* **1970**, *17*, 359.
(30) Cirillo, A.; Fripiat, J. J. *J. Phys.* **1978**, *39*, 247
(31) Bouchy, S. B.; Hamid, D.-A.; Derouane, E. G. *Chem. Commun.* **2000**, 125.

is formed and all the structural motive of MoO_3 is lost. Then, a nontopotactic route would be unavoidable. However, when carbon atoms are available in this early reduction stage, they can take the lattice positions vacated by the leaving oxygen. This carbon incorporation could stabilize the structural motive of MoO_3 and the topotactic transformation is achieved. This simultaneous reduction and carburization at the initial stage of TPR requires the low temperature of the initial reduction and the presence of reactive carbon atoms. These conditions seem to be satisfied by the catalytic effect of the transition metals (Ni, Pd, and Pt) that could activate dihydrogen as well as methane at low temperatures. Other metals (Cu, Co, and Mo_2C) fail to provide the topotactic route because they cannot activate dihydrogen and methane at low enough temperatures where the rate of oxygen removal is not too fast relative to the rate of carbon incorporation. Thus, the difference between Pt, Pd, and Ni, which form the cubic MoC_{1-x}, and Co, Cu, and Mo_2C, which form the hexagonal Mo_2C, is their ability to activate dihydrogen and methane; that is, Co, Cu, and Mo_2C require higher temperatures to become active in dihydrogen and methane dissociation than Pt, Pd, and Ni.

The most significant difference between two types of MoC_{1-x} samples prepared by the direct reduction/carburization (Figure 6) and via Mo_2N (Figure 4) is their morphology. The MoC_{1-x} produced via Mo_2N maintains the platelet morphology of the MoO_3, demonstrating an almost perfect pseudomorphism. These MoC_{1-x} particles contain a large amount of pore which accounts for the high surface area of 193 $m^2\ g^{-1}$. Therefore, they must be highly fragile. The morphology of MoC_{1-x} prepared by the metal-promoted direct reduction/carburization seems to be the broken particles and debris from the original large platelets. The direct route seems to be more severe than the nitride route, giving a more serious lattice mismatch and structural stress that would eventually lead to the breakage of the platelets.

Figure 8 summarizes the representative routes for the transformation of MoO_3 to corresponding carbides by the TPR method.[21] Controlling parameters to affect the TPR routes have been known to be the ramping rate of temperature, flow rate, and composition of reactive gases and the final temperature of the TPR.[20] In addition, we can add effects of the transition metal loading on the direct carburization of MoO_3, showing different effects according to the nature of the metals. The direct routes leading to β-Mo_2C are nontopotactic and involve MoO_2 as the main intermediate. Metals such as Cu, Co, and Mo_2C do not produce a new phase, but give surface areas of produced Mo_2C as high as those for α-MoC_{1-x}. The two-step process of $MoO_3 \rightarrow \gamma$-$Mo_2N \rightarrow \alpha$-MoC_{1-x} is a well-known topotactic route giving fcc molybdenum nitride and carbide with high surface

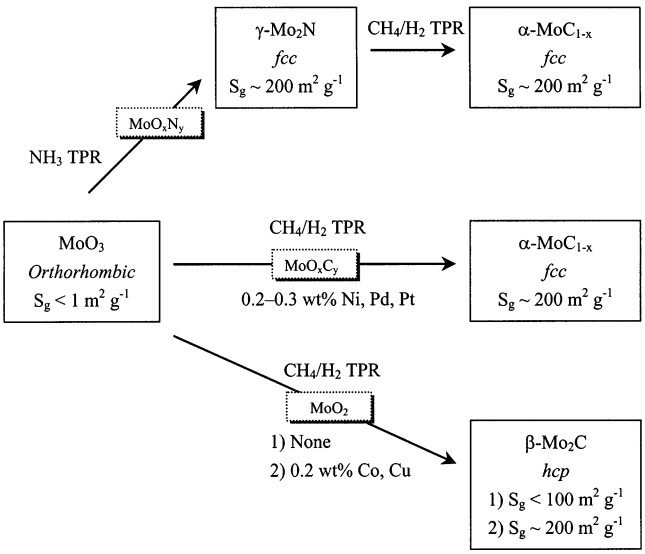

Figure 8. Schematic procedures of the topotactic and nontopotactic transformations of MoO_3 for the synthesis of unsupported molybdenum carbide.

areas. This process involves molybdenum oxynitrides as intermediates.[17] The direct carburization of MoO_3 loaded with Ni, Pd, or Pt leads to a topotactic transformation to fcc α-MoC_{1-x} with high surface areas. The route involves a molybdenum oxycarbide intermediate.

Summary

This work investigated the effects of transition metal loading such as Co, Cu, Ni, Pd, and Pt on the solid-state transformation of MoO_3 under TPR with a $CH_4/4H_2$ stream. All metals lowered the initial reduction temperatures of MoO_3 by at least 100 K and led to the great increase in specific surface areas (up to 221 $m^2\ g^{-1}$) and the amount of CO chemisorption of obtained molybdenum carbides. The addition of Ni, Pd, and Pt resulted in a topotactic route to thermodynamically metastable fcc α-MoC_{1-x} through a molybdenum oxycarbide intermediate. The process is, in general, similar to the well-established topotactic transformations of $MoO_3 \rightarrow Mo_2N \rightarrow \alpha$-$MoC_{1-x}$, but pseudomorphism was only partly maintained. By contrast, the loading of Cu, Co, and presynthesized Mo_2C resulted in the stable hcp β-Mo_2C phase through MoO_2 intermediate-like preparation without metal loading. But the metal loading gave Mo_2C with the greatly increased surface areas.

Acknowledgment. This work has been supported by the Brain Korea-21 program of the Korea Ministry of Education, and the Research Center for Energy Conversion and Storage and the National Nanotechnology program of the Korea Ministry of Science and Technology.

CM030395W